J Appl Electrochem (2007) 37:789–797
DOI 10.1007/s10800-007-9312-6

ORIGINAL PAPER

Electrochemical impedance spectroscopic study of barrier layer thinning in nanostructured aluminium

G. D. Sulka · V. Moshchalkov · G. Borghs · J.-P. Celis

Received: 23 October 2006 / Accepted: 9 February 2007 / Published online: 7 March 2007

Abstract The electrochemical behaviour of electropolished and anodised aluminium was studied by electrochemical impedance spectroscopy (EIS). Freshly electropolished aluminium behaves as a pure capacitor exhibiting Warburg impedance at low frequencies. Storage of the electropolished aluminium, even in an air-tight bottle, results in the reconstruction of a uniform compact barrier layer. The impedance response of a stored electropolished aluminium as well as anodised aluminium after oxide removal, done by chemical etching, exhibits only a capacitive loop in the complex plane. The effect of the oxide layer thickness on the impedance data was investigated for layers formed during anodising at a cell potential of 15 or 23 V. Impedance measurements carried out over a wide range of frequencies gave useful information on the efficiency of the thinning of the barrier layer at the bottom of porous aluminium oxide layers. The rate of thinning of the barrier layer was estimated for samples anodised at different voltage.

G. D. Sulka (✉)
Department of Physical Chemistry and Electrochemistry, Jagiellonian University, Ingardena 3, Krakow 30060, Poland
e-mail: Sulka@chemia.uj.edu.pl

V. Moshchalkov
Department of VSM, Katholieke Universiteit Leuven, Leuven 3000, Belgium

G. Borghs
IMEC, Leuven 3000, Belgium

G. D. Sulka · J.-P.Celis
Department of MTM, Katholieke Universiteit Leuven, Leuven 3000, Belgium

Keywords Aluminium oxide · Barrier layer · Barrier layer thinning · Impedance measurements · Porous alumina

1 Introduction

The physical and chemical characteristics of the electrode/electrolyte interface including electron transfer, mass transport and chemical reactions in an electrochemical system influence the impedance of the interface. Furthermore, the impedance of this interface depends on the charge of species adsorbed or present at the electrode/electrolyte interface, the composition of the electrolyte, and also the texture and nature of the electrodes. Electrochemical impedance spectroscopy (EIS) allows a complete description of such electrode/electrolyte interfaces with equivalent circuits for given electron-transfer reactions under given experimental conditions [1, 2]. For this reason, EIS is a powerful tool for the investigation of aluminium oxide films and electrochemical processes at the oxide film/electrolyte interface [3–9].

Complete AC-impedance measurements on anodised aluminium films were performed by Hitzig and Jüttner [10–12]. They investigated properties of sealed porous aluminium oxide layers and their corrosion behaviour especially under natural environmental conditions. Relatively simple physical models explaining changes in the impedance data were derived for a compact barrier layer and for a perfect porous aluminium layer formed after anodization. The passive and active pit models on an inhomogeneous oxide layer on aluminium were also presented. It is well known that information on porous unsealed oxide films cannot be obtained from EIS measurements due to the short circuiting of the porous oxide by the presence of electrolyte in the pores [3, 5, 13, 14].

However, the electrochemical behaviour of unsealed anodised aluminium, nearly identical to the barrier-type film, can even be represented by a simpler model than the equivalent circuit used for description of the barrier-type layer [3, 13]. Instead of commonly used models, described by an electrical equivalent circuits consisting of series and parallel combinations of resistances and capacitances for an ideal parallel plate capacitor, some researchers have suggested different equivalent circuits [15–19]. These circuits contain, for instance, an inductance [15], a Young impedance [16, 17] or taking into account surface state effects [18]. In recent years, the use of EIS for the investigation of aluminium especially aluminium alloys has increased rapidly. The main focus was an investigation of the corrosion resistance of sealed aluminium used for technical applications [13, 14, 20–22].

The aim of this paper is to present the impedance characteristics of nanostructured anodised aluminium after different steps in its synthesis. The anodization of aluminium was recently applied to the synthesis of materials with a nm-scale porous structure with closed packed cells. The synthesis of such materials usually consists of a few successive steps consisting of anodization and removal of the porous oxide formed during anodization [23]. At the bottom of such anodised aluminium films a barrier layer is formed. The thickness of the barrier layer affects the eventual subsequent deposition of metals into the pores formed during anodization [24]. Recently, some researchers have developed procedures for the thinning of the barrier layer to promote nucleation and growth of metals at the bottom of pores [24, 25]. The development of an effective procedure to thin the barrier layer, and of a method for the evaluation of the thinning process are highly desired. In this paper, nanostructured anodised aluminium obtained after anodising at cell potentials of 15 or 23 V was investigated. Impedance measurements on electropolished aluminium are presented as reference. A thinning method based on anodising was applied to reduce the barrier layer thickness. Since the electrochemical response of the barrier layer in unsealed anodised aluminium is the main contribution to the behaviour of the system during impedance measurements the efficiency of our barrier layer thinning procedure was investigated by EIS.

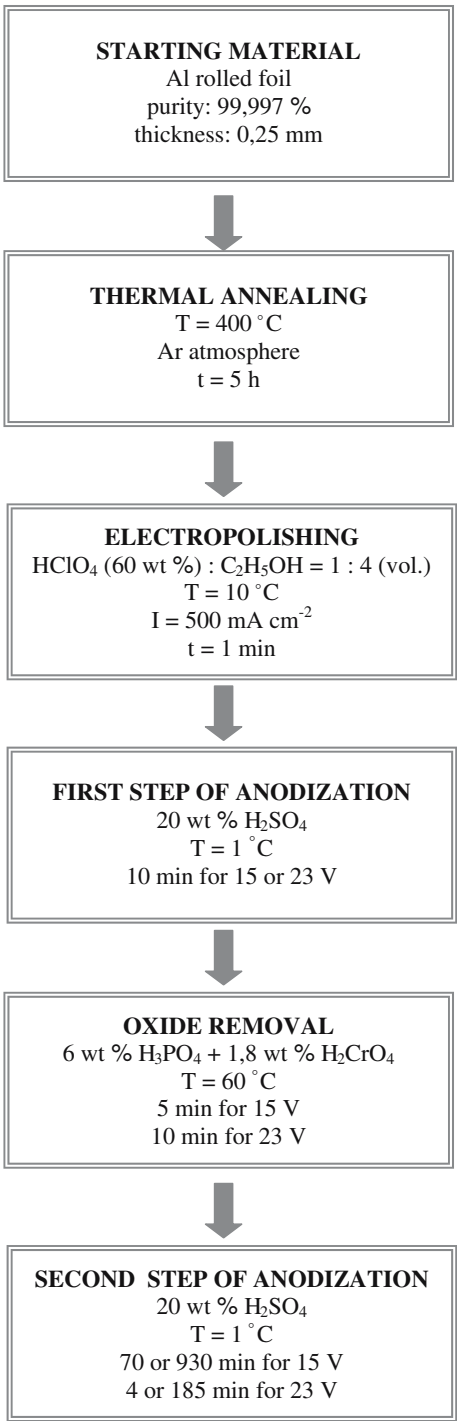

Fig. 1 Experimental procedure for two-step anodization of aluminium

2 Experimental

High purity aluminium foils (99.997%, Alfa Aesar Johnson Matthey GmbH) were pre-treated and anodised at a constant cell potential of 15 or 23 V at 1 °C (Fig. 1). A two-step anodising procedure in 20 wt% sulphuric acid was used [23]. The two-step anodising procedure starts with a short anodising step of 10 min at selected cell potential. Subsequently, removal of the oxide layer was achieved by chemical etching in a mixture of phosphoric acid (6 wt%) and chromic acid (1.8 wt%) at 60 °C. That was followed by a second anodising step at constant cell potential. The duration of the second anodising step was chosen in

view of the desired thickness of the oxide layer. Porous aluminium film thickness of 7.5 or 107 μm were produced at both anodising potentials. The thickness of the porous alumina layers formed after two-step anodising was estimated from SEM-FEG images. A schematic representation of the anodised layer is shown in Fig. 2. SEM-FEG top view of the surface structure of aluminium after the second anodising step at a cell potential of 23 V is shown in Fig. 3. The triangular arrangement of well-ordered nanopores is clearly visible.

In order to reduce the thickness of the barrier layer on two-step anodised aluminium an electrochemical thinning procedure was applied [24]. The thinning method is based on anodising at a constant current density. For the sample anodised at 15 V, one thinning anodization step at a constant current density of 1 mA cm^{-2} was performed. Two thinning anodizations at current densities successively of 4 and 1 mA cm^{-2} were used for samples anodised at 23 V.

The impedance of the system was measured with a Solartron Frequency Analyzer SI 1225 together with a Solartron Electrochemical Interface SI 1287. Measurements were performed at frequencies ranging from 65 kHz to 10 mHz with a constant amplitude of the ac signal of 10 mV. Impedance data were found not to depend on the electrode-potential and the perturbation-signal amplitude in the range of 10–100 mV. A three-electrode cell setup with a saturated sulphate electrode as reference electrode and a platinum grit as counter electrode was used. To reduce phase shift errors at high frequencies a low impedance reference system was established connecting a platinum probe in parallel to the reference electrode by a 2.4 nF capacitance. Tests were carried out in a 0.2 M K_2SO_4 electrolyte of pH 5.9 operated at 25 °C. The exposed surface area of samples was 0.5 cm^2.

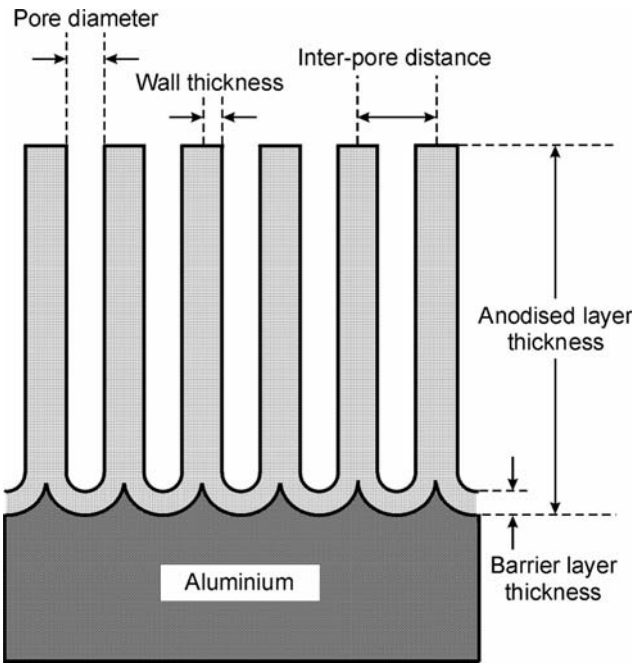

Fig. 2 Porous oxide layer formed on anodised aluminium

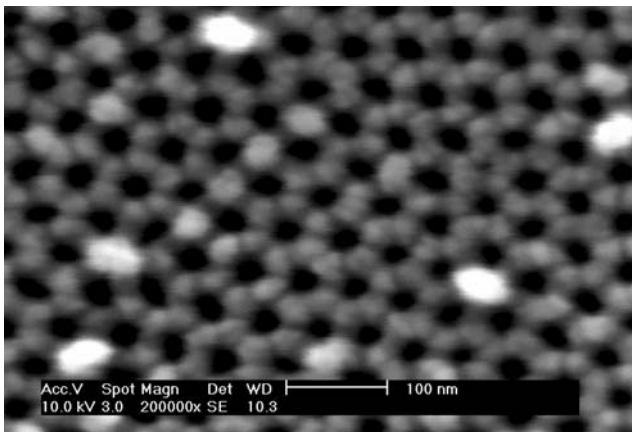

Fig. 3 Secondary electron SEM-FEG top view image of porous alumina layer obtained on the anodised aluminium after a second anodising step at 23 V

3 Results and discussion

Complex plane impedance diagrams, known as Nyquist plots, are shown in Fig. 4A for fresh electropolished aluminium and after 1 week storage in an air-tight bottle. Bode diagrams, |Z| vs log ω and phase angle vs log ω (Fig. 4B and C), are a more convenient way to reveal any frequency dependence of the impedance data especially at high frequencies. As can be seen from Fig. 4, the two electropolished aluminium samples behave as a capacitor system. On a stored electropolished Al sample, a reconstruction of a uniform barrier layer at the surface is observed. The diameter of the semicircle in the complex plane (Fig. 4A) as well as the plateau at low frequencies in the |Z| vs log ω plot (Fig. 4C) correspond to a sum of electrolyte and barrier layer resistances. Additionally a narrowing of the maximum in the phase angle plot (Fig. 4B) is noticed. For the case of a stored electropolished samples, the surface is covered with a passive compact film and a limit in the interfacial reaction appears. The transport of species does not influence the impedance and as a result of an almost purely capacitive response of the system a semicircle appears in Fig. 4A.

Impedance diagrams for aluminium anodised in a first step at 15 or 23 V for 10 min and from which the oxide layer was removed during a chemical etching treatment are shown in Fig. 5. The impedance locus for both samples is located between the corresponding graphs obtained for fresh and stored electropolished aluminium (compare

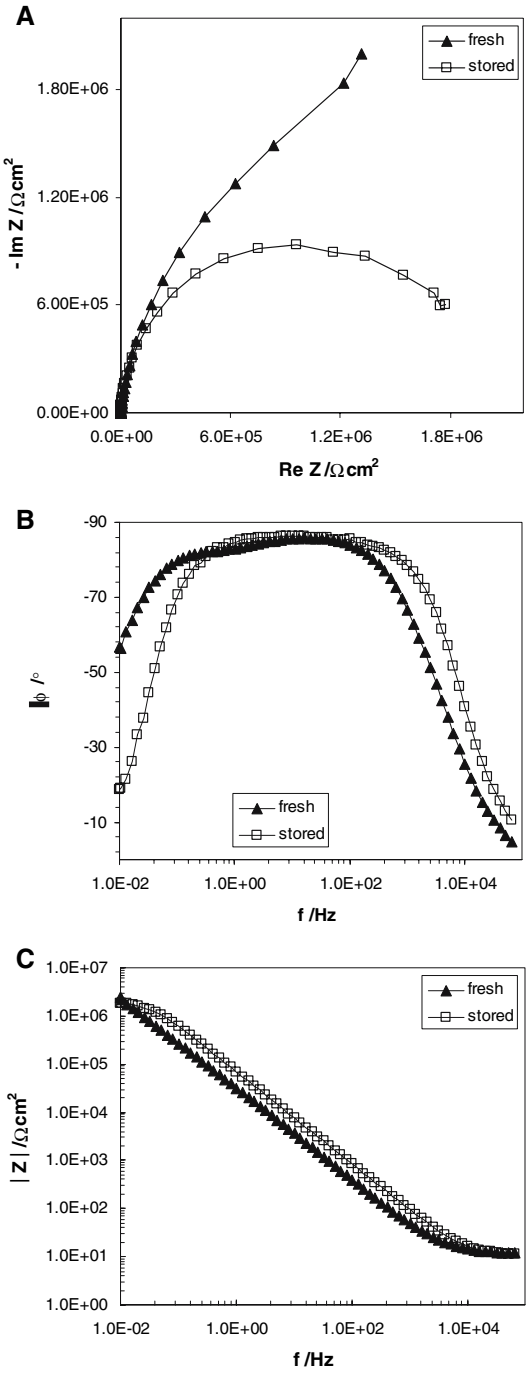

Fig. 4 Complex plane impedance diagram (**A**) and Bode diagrams (**B** and **C**) for a freshly electropolished Al and 1 week stored one

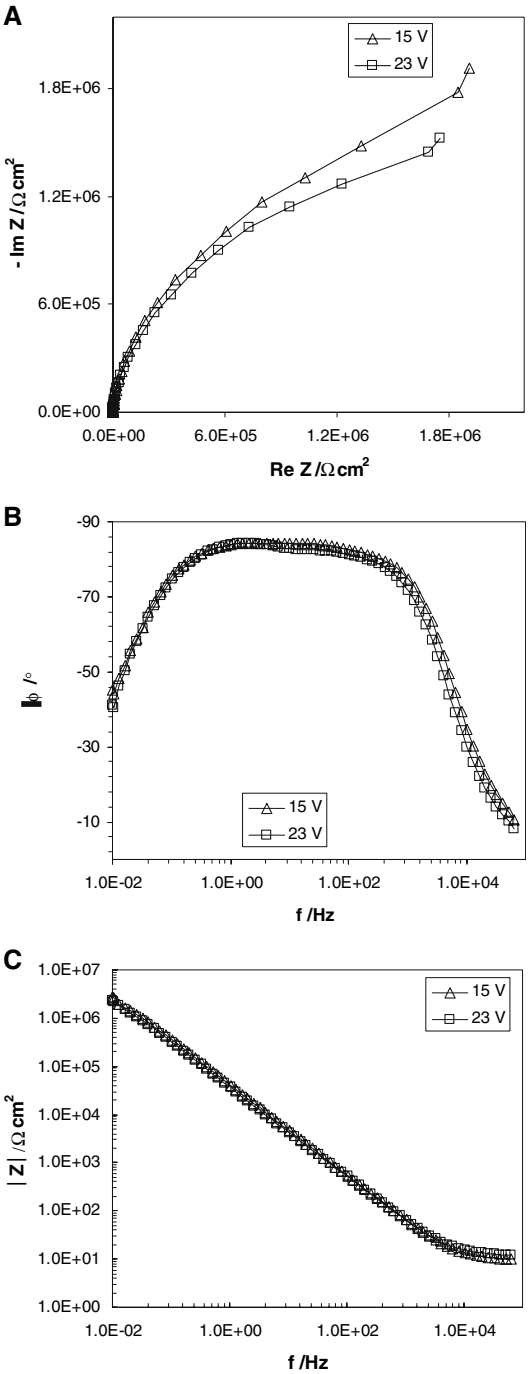

Fig. 5 Complex plane impedance diagram (**A**) and Bode diagrams (**B** and **C**) recorded after an oxide removal by chemical etching on a first step anodised aluminium at 15 or 23 V

Figs. 4A and 5A). From a partially resolved semicircle at high frequencies it can be concluded that the oxide removal procedure is efficient and almost completely removes the anodised film from the aluminium surface. The electrochemical response of samples after oxide removal by chemical etching is similar to that of a freshly electropolished sample. This is confirmed by the lack of a plateau at low frequencies (close to the *Y*-axis) in the Bode diagram (Fig. 5C). Moreover, Bode diagrams recorded for samples obtained by anodising in the first step at a cell potential of 15 or 23 V and then subsequently chemically etched are identical. This means that a very thin oxide layer left on the surface of aluminium after the oxide removal has similar electrochemical characteristics.

It is generally accepted that the barrier layer thickness is proportional to the anodising potential [26] and that it can be estimated on the basis of the following equation:

$$d_b = 1.3V\ [\text{nm}] \quad (1)$$

where V is the anodising cell potential. According to Eq. (1), the thickness of the barrier layer formed during anodising at constant cell potentials of 15 and 23 V, is expected to be about 19.5 and 30 nm, respectively. During the thinning step, which is based on anodization at constant current density the cell potential decreases from 23 or 15 to about 7 V. The potential of 7 V corresponds to a thickness of the barrier layer of only 9 nm. The thinning of the barrier layer during anodization at constant current density is possible due to the higher rate of dissolution of oxide from the barrier layer/solution interface than of oxide formation at the aluminium/barrier layer interface [27]. Moreover, the dissolution rate increases with increase in relative potential drop, D_V, defined as a ratio of the difference between the initial cell potential and the potential at the end of the thinning step to the initial potential. The relative potential drop, D_V, in our experiments was 0.5 and 0.7 at anodising cell potentials of 15 and 23 V respectively.

Complex plane impedance plots and Bode diagrams for aluminium anodised in two steps, as well as for aluminium anodised in two steps and subsequently thinned, are shown in Figs. 6 and 7. For the anodising step in Figs. 6 and 7 potentials of 15 and 23 V were applied, respectively. Two durations of barrier layer thinning for samples previously anodised at a certain cell potential are also indicated in Figs. 6 and 7. The thickness of the oxide layer formed during anodising at these two cell potentials was kept at 7.5 μm. For the case of anodization at 15 V a one-step thinning at a constant current density was applied for 5 or 30 min. On samples anodised at 23 V two successive thinning steps at constant current density were conducted. The total duration of the thinning steps was 8 or 35 min. Figures 6A and 7A reveal that the impedance locus is smaller for thinned samples. The size of the locus decreases with increasing duration of the thinning step. This means that the resistance of the system depends strongly on the barrier layer thickness. Relatively small changes in the barrier layer thickness result in big changes in system resistance. It is generally accepted [e.g. 22] that the porous layer resistance is about six orders of magnitude lower than the associated barrier layer resistance. This indicates that the barrier layer structure is rather dense and compact. A similar tendency of decreasing resistance with increasing duration of the thinning of the barrier layer is observed in Figs. 6C and 7C. On comparing the impedance loci for non-thinned anodised in two steps aluminium at different cell potentials (Figs. 6A and 7A), it becomes evident that the resistance of the system is slightly larger for aluminium anodised at 23 V than at 15 V. This behaviour is consistent with literature results [6, 7]. The inductive loop at low frequencies noticed in Figs. 6A and 7A, indicates a high relaxation time constant of the Faradaic process [1, 28] for thinned samples. The Faradaic impedance is related mainly to processes occurring at the barrier oxide layer/electrolyte interface and is usually explained by processes involving reaction intermediates. The inductive loop at low-frequency in the Nyquist plots (Figs. 6A and 7A) can be explained in terms of different rates of the annihilation and formation of negatively and positively charged vacancies in the oxide layer at the aluminium/oxide film interface. According to Moon and Pyun [8, 9], the low-frequency inductive loop is associated with an ionic relaxation phenomenon within the oxide film. This ionic relaxation phenomenon is due to the variation with time of O^{2-} ion build-up at the aluminium/oxide film interface. This behaviour, as was shown by Moon and Pyun [8, 9], can play a role especially at low current densities (below 10 mA cm^{-2}) where the annihilation rate of negatively charged aluminium vacancies in the oxide exceeds the formation rate of positively charged oxygen vacancies in the oxide at the aluminium/oxide film interface. As a result of this, after filling most of the aluminium vacancies in the oxide layer, aluminium ions can adsorb on the oxide layer at the aluminium/oxide film interface. It can be concluded that adsorption of aluminium ions occurred in our experiments during the thinning of samples at constant current density where a very low current density is involved. The current densities used during the thinning step were 4 and/or 1 mA cm^{-2}. The thinning procedure generally results in a narrowing of plots of phase angle vs frequency (Figs. 6B and 7B). The phase angle goes through a minimum in the middle part of the plot for aluminium anodised in two steps. On thinning, this minimum shifts slightly to higher frequencies. Such a minimum was not observed in the phase angle plot either for electropolished aluminium or anodised samples after oxide removal treatment. These results suggest that the minimum appears in the phase angle plots only when a relatively thick oxide layer is present. As can be seen from the |Z| vs log ω Bode diagram in Figs. 6C and 7C, the resistance of anodised aluminium is higher before than after thinning of the barrier layer. These figures confirm that EIS is a powerful technique that can be used for the study of the efficiency of the thinning of the barrier layer present at the bottom of anodised aluminium.

The complex plane impedance data and Bode diagrams for samples anodised at 15 and 23 V are shown in Fig. 8 for an oxide layer thickness of 107 μm. After a second

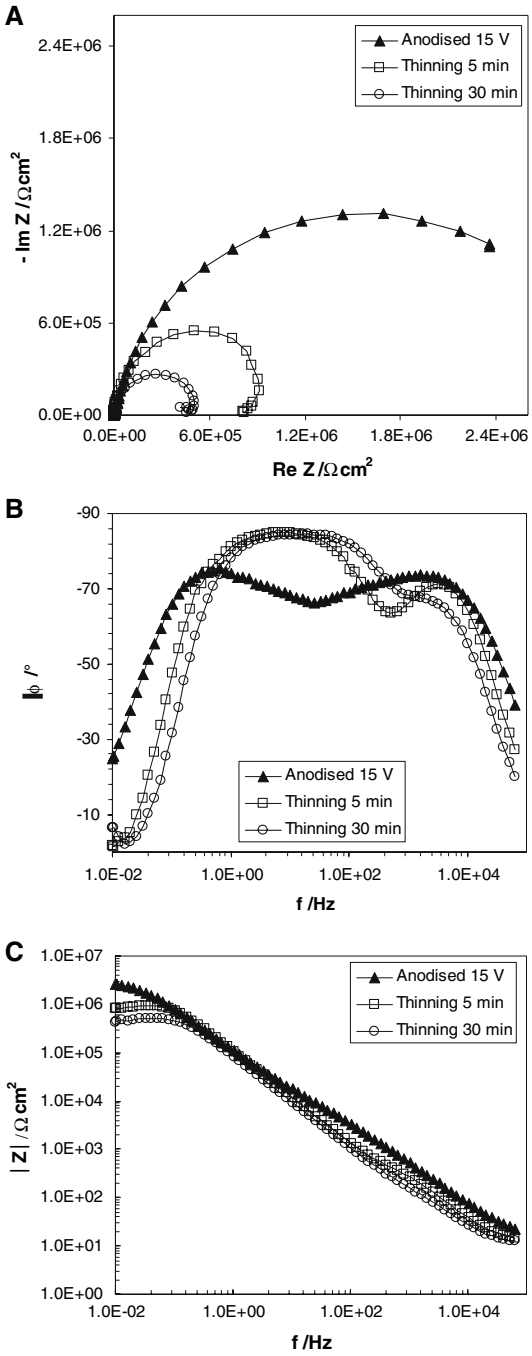

Fig. 6 Complex plane impedance diagram (**A**) and Bode diagrams (**B** and **C**) for a two-steps anodised aluminium before and after thinning of the barrier layer for 5 or 30 min. A two-step anodising was performed at 15 V. The thickness of the oxide layer before thinning was 7.5 μm

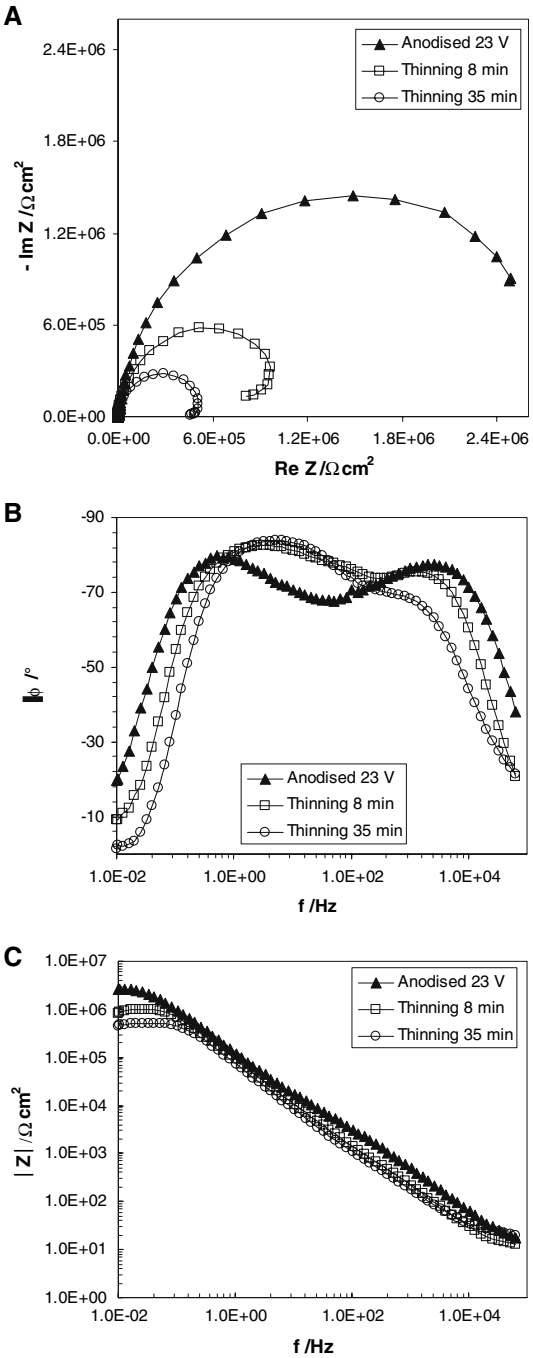

Fig. 7 Complex plane impedance diagram (**A**) and Bode diagrams (**B** and **C**) for a two-steps anodised aluminium before and after thinning of the barrier layer for 5 or 30 min. A two-step anodising was performed at 23 V. The thickness of the oxide layer before thinning was 7.5 μm

anodization step at a given cell potential, one- or two-step thinning procedures were performed in a similar way as on samples presented in Figs. 6 and 7. The total duration of the thinning of the barrier layer was 30 and 35 min on samples anodised at 15 and 23 V, respectively. As can be seen from Fig. 8, the resistive response of the system is similar to that observed in Figs. 6 and 7. A low-frequency inductive loop is observed for both thinned samples. The thinning step significantly reduces the resistance of the system. For samples with a thinned barrier layer, the

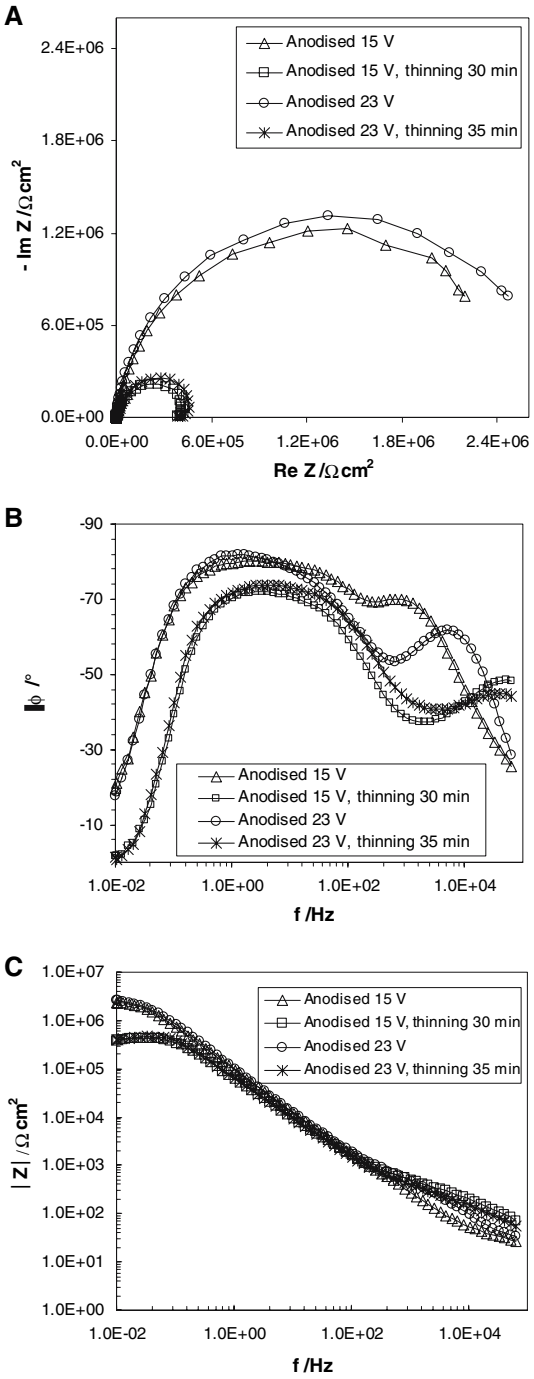

Fig. 8 Complex plane impedance diagram (**A**) and Bode diagrams (**B** and **C**) for a two-steps anodised aluminium produced at 15 and 23 V before and after thinning of the barrier layer. The thickness of the oxide layer was 107 μm

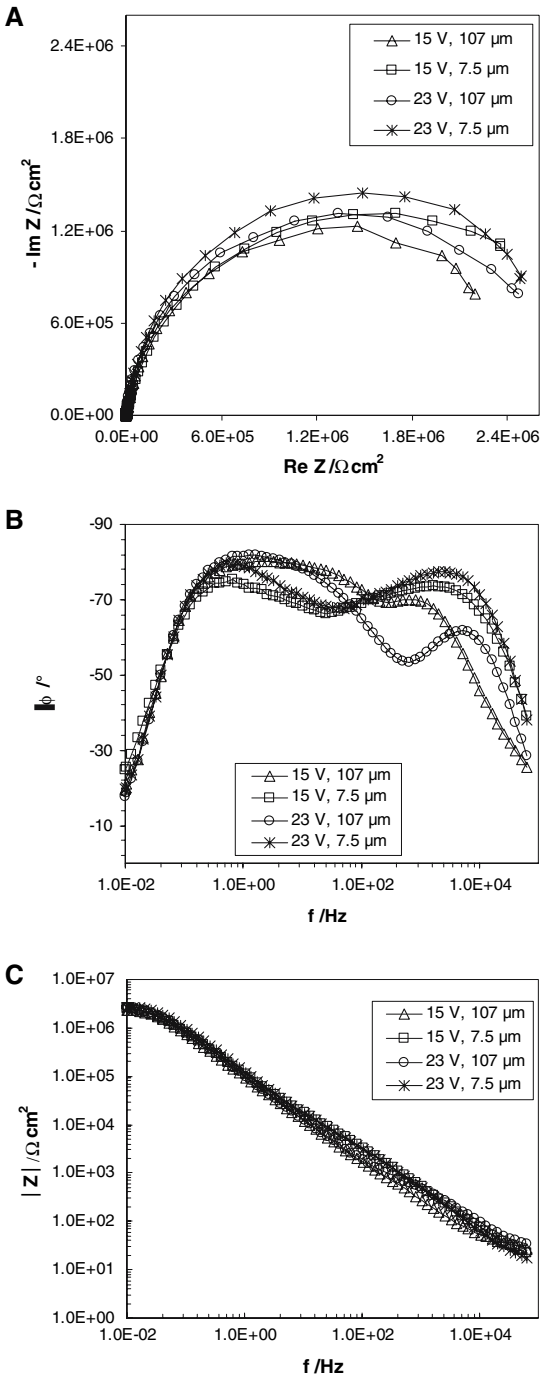

Fig. 9 Complex plane impedance diagram (**A**) and Bode diagrams (**B** and **C**) for two-steps anodised aluminium produced at 15 and 23 V. The thickness of the oxide layer was 7.5 or 107 μm

plateau observed in the Body diagram at low frequencies (Fig. 8C) is stabilized at a lower impedance value. The results obtained on oxide layers of different thickness formed by two-steps anodising at 15 and 23 V are shown in Fig. 9. The thickness of the anodised layer was 7.5 or 107 μm for samples produced at both cell potentials. The analysis of these data reveals, as expected, that the thickness of the porous oxide layer does not significantly modify the electrochemical response of the system.

The experimental barrier film never behaves as an ideal capacitor and exhibits a different constant phase shift from the theoretical value of 90° predicted for an

ideal capacitor. Taking this into account an empirical relation for the barrier layer impedance with an experimental frequency dispersion factor (α) can be written as follows:

$$Z = 1/(j\omega)^{a} C_b \tag{2}$$

where C_b is the capacitance of the barrier layer and Z, ω and j are impedance, angular frequency ($\omega = 2\pi f$) and the unit on the imaginary axis, respectively. The frequency dispersion factor can be calculated from the Bode diagram of phase angle vs log ω. On the other hand, the capacitance of the barrier layer can be easily estimated from the slope of the Bode diagram (|Z| vs. log ω) as was shown by Hitzig and Jüttner [10–12]. This is achieved by extrapolating the high-frequency linear part of the slope to frequency $\omega = 1$. Furthermore, the capacitance is closely related to the thickness of the barrier layer (d_b) according to a plate capacitor relationship:

$$C_b = \varepsilon\varepsilon_0 A_g/d_b \tag{3}$$

where A_g, ε and ε_o represent the geometric surface area, the dielectric constant of aluminium oxide (8.5) and the permittivity of vacuum (8.854×10^{-14} F cm^{-1}), respectively.

From Eqs. (2) and (3), the thickness of the barrier layer was calculated from the experimental data. Values for the barrier layer thickness on anodised samples in two steps at cell potentials of 15 or 23 V were about 5-fold lower than those calculated from Eq. (1). However, it is worth noting that researchers have usually observed higher experimental capacitance of the barrier layer on unsealed anodised aluminium in comparison to sealed anodised aluminium [5, 21].

The percent reduction of the barrier layer thickness, R, was calculated to determine the influence of the thinning duration on the efficiency of the barrier layer thinning for both values of anodising cell potentials (Fig. 10). As mentioned earlier, the relative potential drop, D_V, was 0.7 and 0.5 for samples anodised at 23 and 15 V respectively. A 50% reduction in the barrier layer thickness is observed after about 32 and 40 min of thinning at relative potential drops of 0.7 and 0.5, respectively. This means that thinning of the barrier layer proceeds faster at a lower relative potential drop. These results also show that the applied thinning procedures did not effectively reduce the thickness of the barrier layer on anodised samples, and that the duration of the thinning step has to be extended.

Assuming that the experimental thickness of the barrier layer in anodised aluminium samples equals the value predicted by Eq. (1), and taking into account the estimated percent of reduction of the barrier layer thickness for thinned samples, the remaining thickness of the barrier layer was calculated after a certain time of thinning. The data obtained from these analyses are presented in Fig. 11. The slope of the best fit curve corresponds to the thinning rate of the barrier layer. The thinning rate depends on the relative potential drop and is about 0.44 or 0.26 nm min^{-1} at relative potential drops of 0.7 and 0.5 respectively. These results are consistent with thinning rates obtained by Kim et al. [28] in 0.5 M H_2SO_4. A thinning rate of 0.30 nm min^{-1} was reported by them for a relative potential drop of 0.5. However, the thinning procedure used in this work was not optimum. Notwithstanding this data presented in Figs. 10 and 11 clearly show that an effective reduction of the barrier layer thickness can be achieved by extending the thinning time to about 50 min.

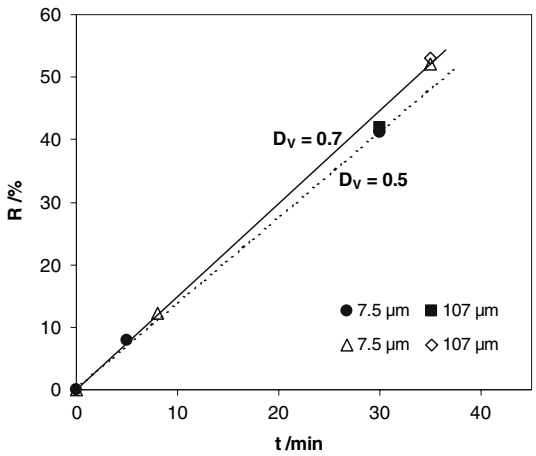

Fig. 10 The thinning efficiency of the barrier layer thickness at various relative potential drops

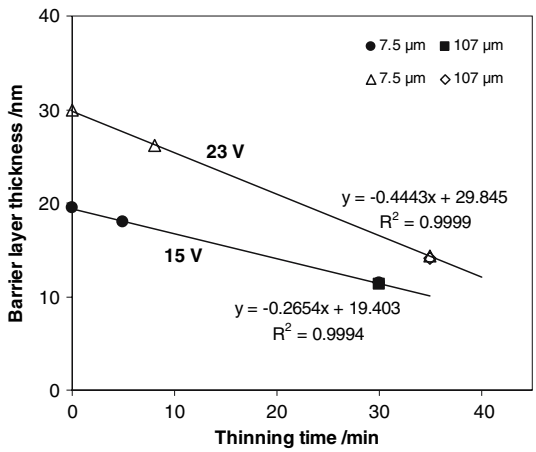

Fig. 11 Variation of the thickness of the barrier layer with thinning time

4 Conclusions

The impedance response of electropolished aluminium before and after oxide removal exhibits a typical capacitance loop originating from the time constant of the charge transfer resistance and the electric double layer capacitance. A low-frequency inductive loop appears in the impedance response of samples after electrochemical thinning of the barrier layer. This suggests partial adsorption of aluminium ions at the aluminium/oxide film interface. The barrier layer thinning procedure used in this study and based on anodising seems to be of low efficiency, but a desired thickness of the barrier layer below 10 nm can be obtained by extending the thinning anodization time above 50 min. The rate of thinning of the barrier layer depends on the anodising cell potential and is about 0.44 or 0.26 nm min^{-1} for samples anodised at 23 and 15 V, respectively.

This study shows that impedance measurements carried out over a wide range of frequencies give useful information on the properties of anodised aluminium. It also allows investigation of the efficiency of the barrier layer thinning procedure.

Acknowledgements This work was funded by the Flemish Science Foundation (contract FWO G.0299.99) and by the Flemish Government (BIL-Poland 00/15).

References

1. Gabrielli C (1981) Identification of electrochemical processes by frequency response analysis, Solartron instruments technical report No 004/83. Farnborough, England
2. Ross Macdonald J (ed) (1987) Impedance spectroscopy emphasizing solid materials and systems. A Wiley – Interscience Publication, John Wiley & Sons, New York
3. Van der Linden B, Terryn H, Vereecken J (1990) J Appl Electrochem 20:798
4. Frichet A, Gimenez P, Keddam M (1993) Electrochim Acta 38:1957
5. De Laet J, Terryn H, Vereecken J (1996) Electrochim Acta 41:1155
6. De Wit JHW, Lenderink HJW (1996) Electrochim Acta 41:1111
7. Dimogerontakis T, Kompotiatis L, Kaplanoglou I (1998) Corros Sci 40:1939
8. Moon S-M, Pyun S-I (1998) Electrochim Acta 43:3117
9. Moon S-M, Pyun S-I (1998) J Solid State Electrochem 2:156
10. Hitzig J, Jüttner K, Lorenz WJ, Paatsch W (1984) Corros Sci 24:945
11. Hitzig J, Jüttner K, Lorenz WJ, Paatsch W (1986) J Electrochem Soc 133:887
12. Jüttner K, Lorenz WJ, Paatsch W (1989) Corros Sci 29:279
13. López V, González JA, Otero E, Escudero E, Morcillo M (2002) Surf Coat Technol 153:235
14. Domingues L, Fernandes JCS, Da Cunha Belo M, Ferreira MGS, Guerra-Rosa L (2003) Corros Sci 45:149
15. Bessone J, Mayer C, Jüttner K, Lorenz WJ (1983) Electrochim Acta 28:171
16. Oh H-J, Jang K-W, Chi Ch-S (1999) Bull Korean Chem Soc 20:1340
17. Oh H-J, Jeong Y, Suh S-J, Kim Y-J, Chi ch-S (2003) J Phys Chem Solids 64:2219
18. Gervasi CA, Vilche JR (1992) Electrochim Acta 37:1389
19. Goeminne G, Terryn H, Vereecken J (1995) Electrochim Acta 40:479
20. Bonnel K, Le Pen C, Pébère N (1999) Electrochim Acta 44:4259
21. Siva Kumar C, Shankar Rao V, Raja VS, Sharma AK, Mayanna SM (2002) Corros Sci 44:387
22. Suay JJ, Giménez E, Rodríguez T, Habbib K, Saura JJ (2003) Corros Sci 45:611
23. Sulka GD, Stroobants S, Moshchalkov V, Borghs G, Celis J-P (2002) J Electrochem Soc 149:D97
24. Nielsch K, Müller F, Li A-P, Gösele U (2000) Adv Mater 13:582
25. Xu D, Xu Y, Chen D, Guo G, Gui L, Tang Y (2000) Chem Phys Lett 325:340
26. Wernick S, Pinner R, Sheasby PG (1987) The surface treatment and finishing of aluminium and its alloys, 5th edn, vol I. ASM International, Finishing Publication LTD, p 289
27. Armstrong RD, Edmondson K (1973) Electrochim Acta 18:937
28. Kim Y-S, Pyun S-I, Moon S-M, Kim J-D (1996) Corros Sci 38:329